Circularly Polarized Substrate Integrated Waveguide Antenna With Wide Axial-Ratio Beamwidth

Yu Luo, *Member, IEEE*, and Jens Bornemann, *Fellow, IEEE*

***Abstract*—A circularly polarized (CP) substrate integrated waveguide (SIW) antenna is presented. First, our study demonstrates that wide axial-ratio beamwidth can be achieved by exciting a square slot with four pins. Second, gap rings are employed around the pins to control the resonant frequency of the antenna. After the variation of thee diameters of gap rings, the frequency of best impedance match corresponds to that of the widest axial-ratio beamwidth. Finally, a CP antenna is designed and fabricated. Experimental results are found in good agreement with simulations in terms of radiation patterns, gain, axial ratio, and reflection coefficient. In particular, the 3-dB axial-ratio beamwidth at the center frequency of 7.98 GHz is extended to 150°.**

***Index Terms*—Axial ratio (AR), cavity antenna, circular polarization, substrate integrated waveguide (SIW).**

I. Introduction

IT IS well known that circularly polarized (CP) radiation represents a powerful tool in reducing polarization mismatch resulting from multipath interference. Hence, various CP antennas have been explored nowadays [1], for many wireless applications. As usual, CP antennas need to be designed with a wide 3-dB axial-ratio (AR) angular beamwidth in order to transmit and receive signals over a wide field of view for airborne communications or satellite communications [2].

Cavity-backed techniques can be used to improve the gain of CP antennas [3]–[6]. However, backing cavities with quarter-wavelength depths limit their applications, and the fabrication is also complicated. Recently, substrate integrated waveguide (SIW)-based CP antennas have been proposed and designed [7]–[11] as a preferred choice over conventional microstrip technology. By employing SIW, the low-profile cavity-backed structure can be realized by using only low-cost printed circuit board (PCB) substrates. Crossed slots, treated as magnetic crossed dipoles, were employed to realize CP radiation [7]–[10]. However, as investigated in [12], wide axial-ratio beamwidths cannot be achieved by crossed dipoles. Four rectangular radiation slots were deployed to achieve CP radiation in the broadside direction [11], but the focus was not on wide axial-ratio beamwidth. Helical antennas, with varied configurations [13]–[14], were designed to obtain 150° or 180° 3-dB AR beamwidths. However, these designs are difficult to be accurately fabricated, especially at high frequencies. Patch antennas on suspended substrates were designed to achieve a 3-dB AR beamwidth as wide as 180° [2] and 120° [15]. However, the suspended substrate configuration increases complexity and increases the height of such antennas. CP antennas comprising two pairs of linear dipoles [12] or folded dipoles [16] in square contours were presented. By adjusting the distance between dipoles, 126° or 135° 3-dB axial-ratio beamwidth is obtained. For both antennas, adjusting the distance between dipoles has less effect on impedance match. Unfortunately, both of the antennas suffer from extremely low front-to-back ratio.

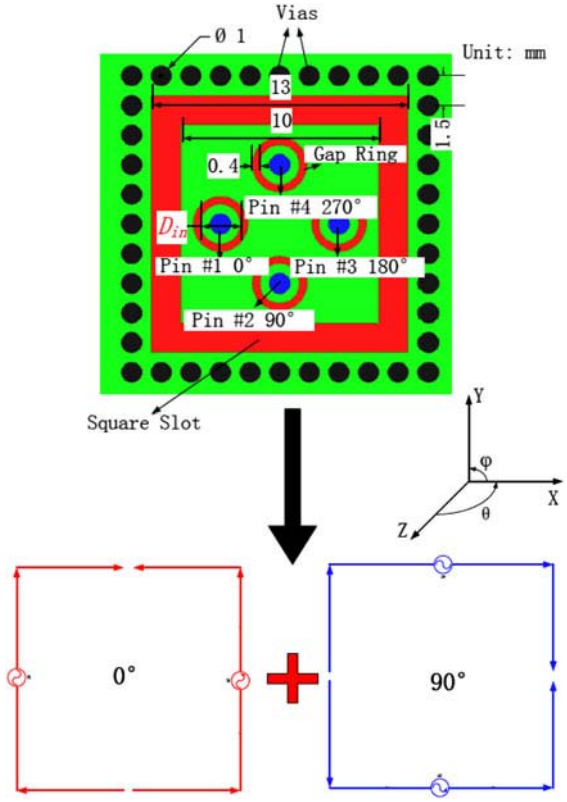

Fig. 1. Square slot on an SIW cavity and its coordinate system.

In this letter, a novel approach to designing an SIW CP antenna with wide AR beamwidth is presented. Four pins are employed to excite a square slot, and they have 90° phase difference between adjacent elements. The antenna can be treated as two pairs of magnetic dipoles in a square contour. Different

Manuscript received February 23, 2016; accepted May 18, 2016. Date of publication May 23, 2016; date of current version February 27, 2017. This work was supported by the National Science and Engineering Research Council of Canada.

The authors are with the Department of Electrical and Computer Engineering, University of Victoria, Victoria, BC V8W 2Y2, Canada (e-mail: yluo@uvic.ca; j.bornemann@ieee.org).

Color versions of one or more of the figures in this letter are available online at http://ieeexplore.ieee.org.

Digital Object Identifier 10.1109/LAWP.2016.2571658

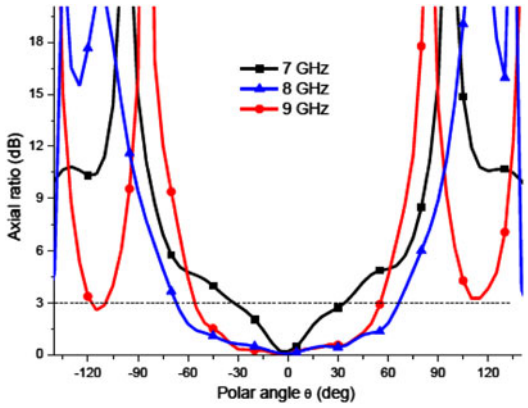

Fig. 2. Simulated axial ratio of the square slot shown in Fig. 1 as a function of polar angle θ in the xz-plane at different frequencies.

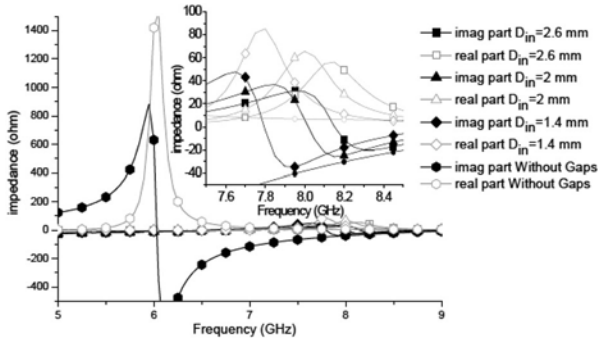

Fig. 3. Effects of gap rings on input impedance.

from the cases in [12] and [16], however, the resonant frequency of the proposed antenna is dependent on the distance between dipoles. This leads to the inconformity between the frequency with best impedance match and the frequency with widest axial-ratio beamwidth. To solve this problem, gap rings are employed to adjust the operating frequency of the antenna without affecting the axial-ratio beamwidth. Thus, the frequency with best impedance match corresponds to that of the widest axial ratio if the diameters of the gap rings are correctly selected. Such an SIW CP antenna is designed and prototyped. Measurements show good agreement with simulations, and a 150° 3-dB axial-ratio beamwidth is achieved.

II. Antenna Design

A square slot with an SIW cavity on a Rogers 5880 substrate with relative permittivity of $\varepsilon_r = 2.2$ and thickness of 1.575 mm is shown in Fig. 1, top. The slot is excited by four pins that are excited with the same amplitude and 90° phase difference between adjacent elements. In this way, the slot can be treated as two pairs of bent magnetic dipoles in a square contour as shown in Fig. 1, bottom. As investigated in [12], if the distance between dipoles, i.e., the length of the side of the square slot, is correctly chosen, a wide-beam axial ratio can be achieved. The axial ratios, simulated by HFSS [17], as a function of polar angle θ in the xz-plane at different frequencies, are shown in Fig. 2. At 8 GHz, widest 3-dB axial-ratio beamwidth is obtained.

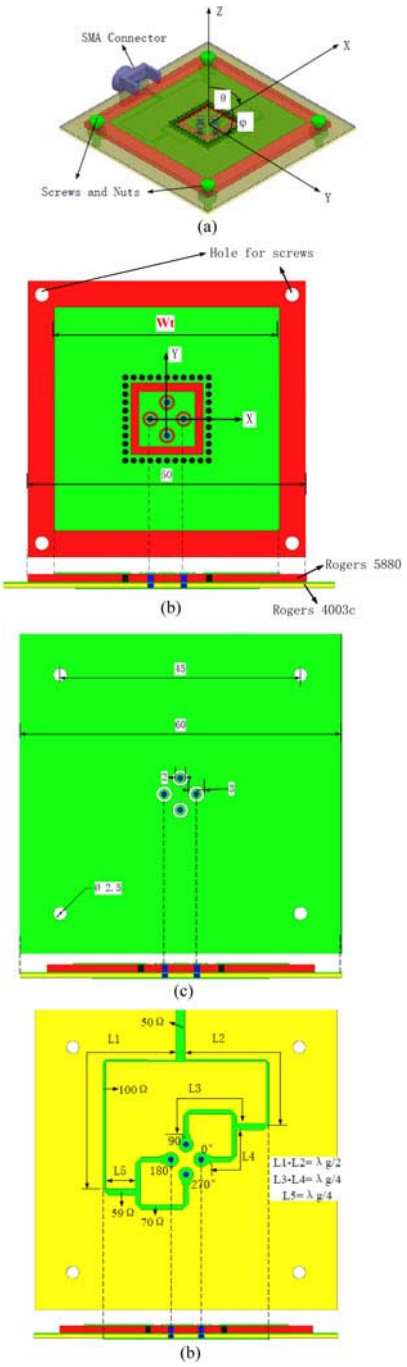

Fig. 4. Geometry of the proposed SIW CP antenna. (a) Three-dimension model. (b) Radiator on the top surface. (c) Ground plane surface. (d) Feeding network on the bottom surface.

In order to obtain a good performance of the antenna, impedance matching at the same frequency is also required. Four gap rings are employed to adjust and improve impedance matching. The inner diameter of the gap rings is set as D_{in} (Fig. 1). When the square is excited, the symmetry plane (yz-plane) can be treated as a perfect E-plane because pin #1 and pin #3 are excited with the same amplitude but out of phase. Therefore, and to reduce simulation complexity while maintaining accuracy, only half of the antenna is excited by pin #1

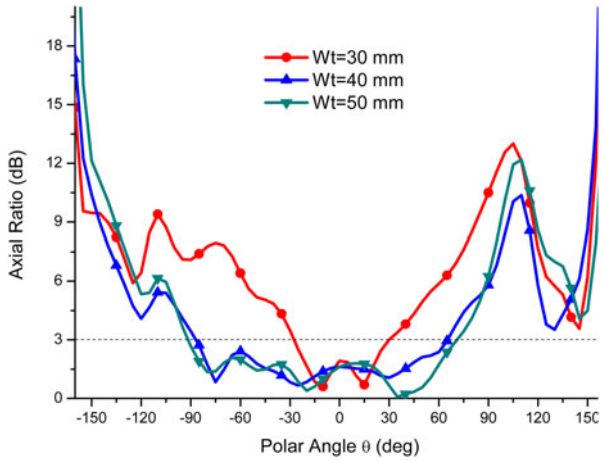

Fig. 5. Effect of W_t on axial ratio over a wide angle range.

with a perfect electric wall in the symmetry plane when calculating the input impedance. The effects of the gap rings on input impedance are shown in Fig. 3. Without gap rings, the resonant frequency (when the imaginary part of the input impedance vanishes) is 6 GHz, which is not equal to the frequency of the widest AR beamwidth. After the addition of gap rings, the resonant frequency is changed and can be controlled. It increases with decreasing D_{in}. When $D_{\text{in}} = 1$ mm, the resonant frequency is almost identical to that of the widest AR beamwidth.

III. Design and Implementation of an SIW CP Antenna

According to the discussion in Section II, a CP antenna consisting of a square slot with SIW cavity is designed and constructed. Fig. 4 shows its geometry. To excite the four pins, a feeding network is designed and printed on Rogers 4003C substrate with relative permittivity of $\varepsilon_r = 3.55$ and thickness of 0.813 mm as shown in Fig. 4(d). λ_g is the guided wavelength. The widths of the 50-, 59-, 70-, and 100-Ω microstrip lines are 1.8, 1.35, 0.95, and 0.45 mm, respectively. The feeding network, designed following previous work in [16], excites the four pins with the same amplitude and 90° phase difference between adjacent elements.

The size of the metallization on the top substrate is set as W_t, and its effect on the axial ratio over a wide angle range is investigated in Fig. 5. With increasing W_t, the axial-ratio beamwidth becomes wider up to $W_t = 40$ mm. Beyond 40 mm, the axial ratio keeps fairly constant with W_t over a wide angle range. To achieve a small size of the entire antenna, $W_t = 40$ mm is selected. In order to fit alignment screws [see Fig. 6(a)], the top substrate size is 50×50 mm^2. The bottom substrate size is slightly larger (60×60 mm^2) to allow for soldering of the SMA connector [see Fig. 6(b)].

To verify the design procedure, we first repeat the simulation in CST [18] and then fabricate and measure the proposed antenna. Fig. 6 depicts photographs of the top and bottom views of the prototype. Measurements of the reflection coefficient, axial ratio, gains, and radiation patterns are performed by using an ANRITSU 37397C Vector Network Analyzer and a far-field antenna test chamber. Experimental results together with simulations in both CST and HFSS are shown in Figs. 7–9. Good agreement between experiments and simulations is observed. Fig. 7 depicts the simulated and measured AR at the center frequency, i.e., 7.98 GHz, as a function of polar angle θ. As predicted in simulations, the measured 3-dB AR beamwidth reaches a value of 150°. As shown in Fig. 8, directive

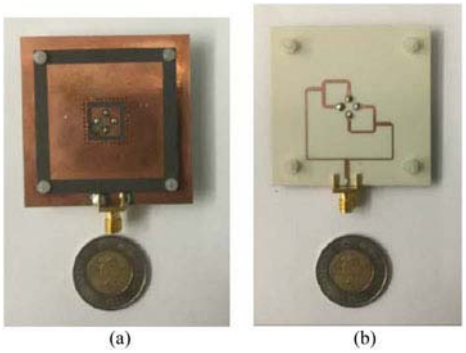

Fig. 6. (a) Top-view and (b) bottom-view photographs of the fabricated antenna and size comparison to a Canadian $2 coin.

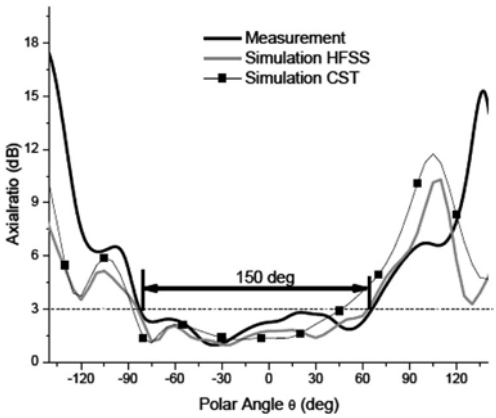

Fig. 7. Simulated and measured axial ratios of the antenna in Fig. 5 in the xz-plane with respect to polar angle θ at 7.98 GHz.

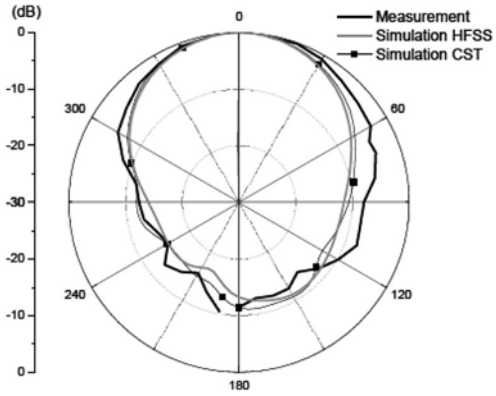

Fig. 8. Simulated and measured normalized radiation patterns in the xz-plane at 7.98 GHz.

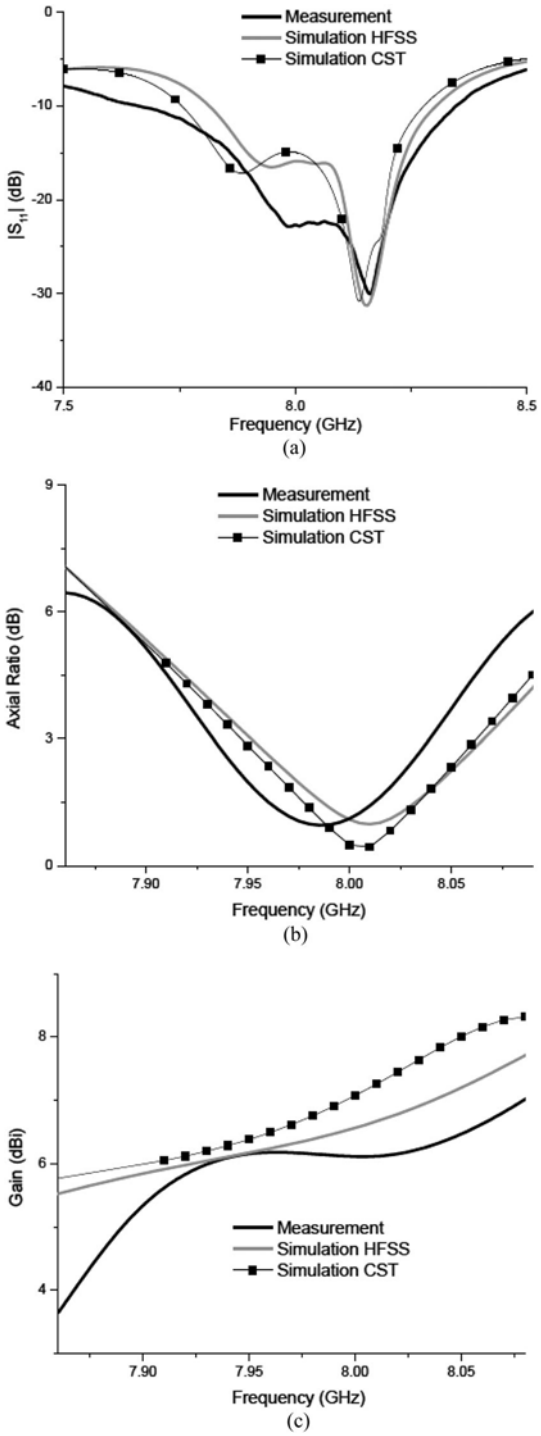

Fig. 9. Simulated and measured antenna parameters as a function of frequency. (a) Reflection coefficient. (b) Axial ratio. (c) Gain in broadside direction, i.e., z-axis.

radiation patterns with 12 dB front-to-back ratio are obtained by the proposed antenna at the center frequency.

Fig. 9(a)–(c) shows the reflection coefficient, AR and gain, respectively, as a function of frequency. The measured gain is better than 6 dBi, and the measured return loss is better than 23 dB at the center frequency. Generally, good agreement between experimental and simulated results is observed.

IV. Conclusion

An SIW CP antenna with wide AR beamwidth is proposed, designed and experimentally verified. The principle of wide AR beamwidth achieved by a square slot is intuitively explained, and four gap rings are employed to adjust the resonant frequency and obtain conformity between the frequencies with best impedance match and widest axial-ratio beamwidth. As shown in both simulation and experiment, the 3-dB axial ratio of the proposed SIW CP antenna can cover an extremely wide angular range with beamwidth of about 150°. Moreover, all other measured results, such as reflection coefficient, radiation gain, and axial ratio, are in good agreement with predictions, thus validating the design approach.

References

[1] S. Gao, Q. Luo, and F. Zhu, *Circularly Polarized Antennas*. New York, NY, USA: Wiley, Nov. 2013.

[2] X. Chen, L. Yang, J. Y. Zhao, and G. Fu, "High-efficiency compact circularly polarized microstrip antenna with wide beamwidth for airborne communication," *IEEE Antennas Wireless Propag. Lett.*, vol. 15, pp. 1518–1521, 2016.

[3] J. Hirokawa, H. Arai, and N. Goto, "Cavity-backed wide slot antenna," *IEE Proc., Microw., Antennas Propag.*, vol. 136, no. 1, pp. 29–33, Feb. 1989.

[4] D. Sievenpiper, H. P. Hsu, and R. M. Riley, "Low-profile cavity-backed crossed-slot antenna with a single-probe feed designed for 2.34-GHz satellite radio applications," *IEEE Trans. Antennas Propag.*, vol. 52, no. 3, pp. 873–879, Mar. 2004.

[5] R. Li *et al.*, "Development of a cavity-backed broadband circularly polarized slot/strip loop antenna with a simple feeding structure," *IEEE Trans. Antennas Propag.*, vol. 56, no. 2, pp. 312–318, Feb. 2008.

[6] W. Yang and J. Zhou, "Wideband circularly polarized cavity-backed aperture antenna with a parasitic square patch," *IEEE Antennas Wireless Propag. Lett.*, vol. 13, pp. 197–200, 2014.

[7] G. Q. Luo, Z. F. Hu, Y. Liang, L. Y. Yu, and L. L. Sun, "Development of low profile cavity backed crossed slot antennas for planar integration," *IEEE Trans. Antennas Propag.*, vol. 57, no. 10, pp. 2972–2979, Oct. 2009.

[8] C. Jin, Z. Shen, R. Li, and A. Alphones, "Compact circularly polarized antenna based on quarter-mode substrate integrated waveguide sub-array," *IEEE Trans. Antennas Propag.*, vol. 62, no. 2, pp. 963–967, Feb. 2014.

[9] A. Elboushi, O. M. Haraz, and A. R. Sebak, "Circularly-polarized SIW slot antenna for MMW applications," in *Proc. IEEE Int. Symp. Antennas Propag. Soc.*, Jul. 2013, pp. 648–649.

[10] G. Zhang and Z. X. Xu. "Development of circularly polarized antennas based on dual-mode hexagonal SIW cavity," in *Proc. 15th Int. Conf. Electron. Packag. Technol.*, Aug. 2014, pp. 1283–1286.

[11] Z. C. Hao, X. M. Liu, X. P. Huo, and K. K Fan, "Planar high-gain circularly polarized element antenna for array applications," *IEEE Trans. Antennas Propag.*, vol. 63, no. 5, pp. 1937–1948, May 2015.

[12] Y. Luo, Q. X. Chu, and L. Zhu, "A low-profile wide-beamwidth circularly-polarized antenna via two pairs of parallel dipoles in a square contour," *IEEE Trans. Antennas Propag.*, vol. 63, no. 3, pp. 931–936, Mar. 2015.

[13] M. Caillet, M. Clénet, A. Sharaiha, and Y. M. M. Antar, "A broadband folded printed quadrifilar helical antenna employing a novel compact planar feeding circuit," *IEEE Trans. Antennas Propag.*, vol. 58, no. 7, pp. 2203–2209, Jul. 2010.

[14] K. Ding, Y. Wang, and X. Xiong, "A novel wide-beam circularly polarized antenna for SDARS applications," *IEEE Antennas Wireless Propag. Lett.*, vol. 11, pp. 811–813, 2012.

[15] N. W. Liu, L. Zhu, and W.-W. Choi, "A low-profile wide-beamwidth circularly-polarized patch antenna on a suspended substrate," *Microw., Antennas Propag.*, vol. 10, no. 8, pp. 885–890, Jun. 2016.

[16] Y. Luo, Q. X. Chu, and L. Zhu, "A miniaturized wide-beamwidth circular polarized planar antenna via two pairs of folded dipoles in a square contour," *IEEE Trans. Antennas Propag.*, vol. 63, no. 8, pp. 3753–3759, Aug. 2015.

[17] AnsoftCorp. HFSS (2008) [Online]. Available: http://www.ansoft.com/products/hf/hfsss

[18] CST studio suite – EM simulation software (2011). [Online]. Available: http://www.cst.com/Content/Products/CST_S2/Overview.aspx